

Doping Dependence of Normal-State Properties in Iron-Based Oxypnictide Superconductor LaFeAsO_{1-y} Probed by ^{57}Fe -NMR and ^{75}As -NMR/NQR

Hidekazu Mukuda^{1,4*}, Nobuyuki Terasaki¹, Nobukatsu Tamura¹, Hiroaki Kinouchi¹, Mitsuharu Yashima^{1,4}, Yoshio Kitaoka¹, Kiichi Miyazawa², Parasharam M. Shirage², Shinnosuke Suzuki³, Shigeki Miyasaka^{3,4}, Setsuko Tajima^{3,4}, Hijiri Kito^{2,4}, Hiroshi Eisaki^{2,4}, and Akira Iyo^{2,4}

¹Graduate School of Engineering Science, Osaka University, Toyonaka, Osaka 560-8531

²National Institute of Advanced Industrial Science and Technology (AIST), Umezono, Tsukuba 305-8568

³Department of Physics, Graduate School of Science, Osaka University, Toyonaka, Osaka 560-0043

⁴JST, TRIP (Transformative Research-Project on Iron Pnictides), Chiyoda, Tokyo 102-0075

We report systematic ^{57}Fe -NMR and ^{75}As -NMR/NQR studies on an underdoped sample ($T_c = 20$ K), an optimally doped sample ($T_c = 28$ K), and an overdoped sample ($T_c = 22$ K) of oxygen-deficient iron (Fe)-based oxypnictide superconductor LaFeAsO_{1-y} . A microscopic phase separation between superconducting domains and magnetic domains is shown to take place in the underdoped sample, indicating a local inhomogeneity in association with the density distribution of oxygen deficiencies. As a result, $1/T_1T$ in the normal state of the superconducting domain decreases significantly upon cooling at both the Fe and As sites regardless of the electron-doping level in LaFeAsO_{1-y} . On the basis of this result, we claim that $1/T_1T$ is not always enhanced by antiferromagnetic fluctuations close to an antiferromagnetic phase in the underdoped superconducting sample. This contrasts with the behavior in hole-doped $\text{Ba}_{0.6}\text{K}_{0.4}\text{Fe}_2\text{As}_2$ ($T_c = 38$ K), which exhibits a significant increase in $1/T_1T$ upon cooling. We remark that the crucial difference between the normal-state properties of LaFeAsO_{1-y} and $\text{Ba}_{0.6}\text{K}_{0.4}\text{Fe}_2\text{As}_2$ originates from the fact that the relevant Fermi surface topologies are differently modified depending on whether electrons or holes are doped into the FeAs layers.

KEYWORDS: superconductivity, iron-based oxypnictide, LaFeAsO , NMR

1. Introduction

The discovery of superconductivity (SC) in the iron (Fe)-based oxypnictide $\text{LaFeAsO}_{1-x}\text{F}_x$ with SC transition temperature $T_c=26$ K has attracted considerable interest in the fields of condensed-matter physics and materials science.¹ Soon after this discovery, the T_c of $\text{LaFeAsO}_{0.89}\text{F}_{0.11}$ was reported to increase up 43 K upon applying pressure,² and the replacement of the La site by other rare-earth (RE) elements significantly increases T_c to more than 50 K.³⁻⁶ The structure of the mother material contains alternately stacked RE_2O_2 and Fe_2As_2 layers along the c -axis, where the Fe atoms of the FeAs layer are located in a fourfold coordination forming a FeAs_4 tetrahedron. The mother material LaFeAsO is a semimetal with a stripe antiferromagnetic (AFM) order with $\mathbf{Q} = (0, \pi)$ or $(\pi, 0)$.⁷ The substitution of fluorine for oxygen and/or oxygen deficiencies in the LaO layer yields a novel SC.^{1, 3-6} Remarkably, Lee *et al.* found that T_c increases to a maximum value of 54 K when the FeAs_4 tetrahedron is transformed into a regular tetrahedron.⁸ Related to this fact, Shirage *et al.* revealed that the a -axis length, corresponding to the distance among Fe atoms in the square lattice, also has a strong correlation with T_c in the RE-Fe-As-O system, as presented in Fig. 1.⁹

In the normal state of $\text{LaFeAsO}_{1-x}\text{F}_x$, pseudogap-like behavior was first reported on the basis of photoemission,¹⁰ ^{75}As -NMR,¹¹ and ^{19}F -NMR¹² measurements. Similar behavior was also reported by ^{75}As -NMR probe for the electron-doped superconductor

$\text{Ba}(\text{Fe}_{0.895}\text{Co}_{0.105})_2\text{As}_2$,¹³ but not for the hole-doped $\text{Ba}_{1-x}\text{K}_x\text{Fe}_2\text{As}_2$.^{14, 15} This suggests that the decrease of ^{75}As -NMR- $(1/T_1T)$ upon cooling, or pseudogap-like behavior, may characterize the normal-state properties in electron-doped Fe-pnictide systems. However, it has been reported by Nakai *et al.*^{11, 16} that ^{75}As -NMR- $(1/T_1T)$ is markedly enhanced upon cooling for underdoped $\text{LaFeAsO}_{1-x}\text{F}_x$ ($x = 0.04$). In addition, they observed a peak at ~ 30 K in $1/T_1$, below which the ^{75}As -NMR spectral width starts to broaden gradually upon cooling.

In this paper, we report systematic studies on the doping dependence of the normal-state properties of electron-doped superconductors LaFeAsO_{1-y} by means of ^{57}Fe -NMR and ^{75}As -NMR/NQR measurements. A microscopic phase separation between SC and magnetic domains is demonstrated to take place in an underdoped sample, indicating a local inhomogeneity in association with the density distribution of oxygen deficiencies. As a result, it is highlighted that $1/T_1T$ at both the Fe and As sites decreases markedly upon cooling, even in SC domains close to an AFM phase, and hence this behavior is a common feature regardless of electron-doping level. This, however, differs from the drastic doping dependence previously observed for ^{75}As -NMR- $(1/T_1T)$, which is markedly enhanced upon cooling in the underdoped sample.¹⁶ We also address the crucial difference observed between the normal-state properties of LaFeAsO_{1-y} and $\text{Ba}_{0.6}\text{K}_{0.4}\text{Fe}_2\text{As}_2$.

*E-mail address: mukuda@mp.es.osaka-u.ac.jp

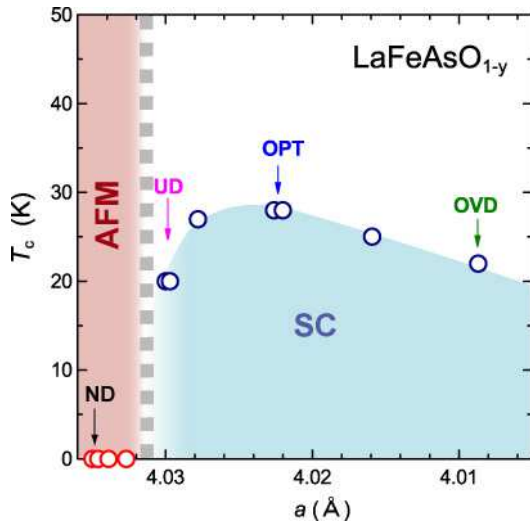


Fig. 1. (color online) Phase diagram of LaFeAsO_{1-y} as a function of a -axis length evaluated at room temperature. An AFM-to-SC transition appears to take place at an a -axis length of approximately $a \simeq 4.03\text{\AA}$, since bulk SC was not obtained in the sample with $a > 4.03\text{\AA}$. In the SC phase, note that even though the nominal oxygen content is different, T_c is almost the same if the a -axis length is identical.

Table I. T_c and lattice parameters at room temperature for a nondoped sample (ND), an underdoped sample (UD), an optimally doped sample (OPT), and an overdoped sample (OVD) of LaFeAsO_{1-y} . Note that T_c can be almost exactly reproduced when the a -axis length is identical, even though the nominal oxygen content is different.

Sample	T_c [K]	a [\AA]	c [\AA]	References
ND	LaFeAsO †	-*	4.0346	8.752
UD	LaFeAsO $_{0.78}^\dagger$	20	4.0300	8.7136
	LaFeAsO $_{0.75}$	20	4.0297	8.7143
OPT	LaFeAsO $_{0.7}^\dagger$	28	4.0226	8.7065 ¹⁷⁾
	LaFeAsO $_{0.6}$	28	4.0220	8.7110 ¹⁸⁾
OVD	LaFeAsO $_{0.6}^\dagger$	22	4.0087	8.6978

†) ^{57}Fe -enriched sample.

$^*)T_N \sim 145$ K.

2. Experimental

Polycrystalline samples of LaFeAsO_{1-y} were synthesized via a high-pressure synthesis technique described elsewhere.⁴⁾ In particular, starting materials of LaAs, ^{57}Fe , and $^{57}\text{Fe}_2\text{O}_3$ enriched by the ^{57}Fe isotope (^{57}Fe : nuclear spin $I = 1/2$, $^{57}\gamma_n/2\pi = 1.3757$ MHz/T) were mixed at a nominal composition of LaFeAsO_{1-y} . Powder X-ray diffraction measurements indicate that these samples are almost entirely composed of a single phase, even though the oxygen content of the samples differs from the nominal content, depending on the oxidation of the starting RE elements. In fact, the SC transition temperature (T_c) for all samples was uniquely determined by a susceptibility measurement, which exhibits a marked decrease due to the onset of SC diamagnetism. There is a strong correlation between T_c and the a -axis length in RE-Fe-As-O systems.⁹⁾ As summarized in Table I and Fig. 1, the T_c of LaFeAsO_{1-y} is almost the same if the

a -axis length is identical regardless of the process used to prepare samples. Bulk SC was not obtained in the sample with $a > 4.03\text{\AA}$. ^{57}Fe -NMR and ^{75}As -NMR/NQR measurements were carried out on an underdoped sample (UD), an optimally doped sample (OPT), and an overdoped sample (OVD) with $T_c = 20$ K, 28 K, and 22 K, respectively. All samples were moderately crushed into powder. The nuclear spin-lattice relaxation rate $1/T_1$ was measured by the saturation-recovery method.

3. Results

3.1 ^{57}Fe -NMR study on LaFeAsO_{1-y}

Figure 2 shows ^{57}Fe -NMR spectra obtained by sweeping the frequency (f) at magnetic field $H = 11.97$ T at 30 K for (a) UD, (b) OPT,¹⁷⁾ and (c) OVD of LaFeAsO_{1-y} . For OPT, which was oriented along the direction including the ab -plane, we observed a single narrow peak when H was applied parallel to the orientation direction, as shown in Fig. 2(b).¹⁷⁾ In the field perpendicular to the orientation direction, two horn-shaped peaks were observed, which arise from crystals with $\theta = 90$ and 0° , where θ is the angle between the field and the c -axis of the crystal. Such a spectral shape originates from the anisotropy of the Knight shift with $^{57}K^\perp \sim 1.413\%$ and $^{57}K^\parallel \sim 0.50\%$ at 30 K for $\theta = 90$ and 0° , respectively.¹⁷⁾ For UD, the ^{57}Fe -NMR spectral width at 30 K is broader than that for OPT, even though it is as narrow as that for OPT at 200 K (see Fig. 10(a)). This suggests that the broad spectrum at 30 K for UD with the field parallel to the ab -plane is ascribed to the distribution of the ^{57}Fe -NMR Knight shift. Figure 2(c) shows the spectrum of nonoriented OVD, which has an asymmetric powder pattern due to the anisotropy of the ^{57}Fe -NMR Knight shift, as corroborated by the ^{75}As -NMR spectrum (see Fig. 5(c)). The temperature (T) dependence of the ^{57}Fe Knight shift was precisely measured for OPT as reported in the literature,¹⁷⁾ but not for UD and OVD because of their broad NMR spectral width. Thus, we focus on the nuclear relaxation behavior to unravel the doping dependence of the normal-state properties in LaFeAsO_{1-y} .

The $^{57}(1/T_1)$ of ^{57}Fe was measured at $H=11.97$ T along the ab -plane ($\theta = 90^\circ$) for all samples. As shown in Fig. 3, $^{57}T_1$ was almost uniquely determined over the entire T range from a single exponential function of $^{57}m(t)_{\text{NMR}}$, which is given by

$$^{57}m(t)_{\text{NMR}} \equiv \frac{M(\infty) - M(t)}{M(\infty)} = \exp\left(-\frac{t}{T_1}\right),$$

where $M(\infty)$ and $M(t)$ are the respective nuclear magnetizations for the thermal equilibrium condition and at time t after the saturation pulse.

Figure 4 shows the T dependences of ^{57}Fe - $(1/T_1T)$ for UD, OPT,¹⁷⁾ and OVD. In the normal state, $1/T_1T$ decreases significantly upon cooling for all samples, and the magnitude of $1/T_1T$ decreases markedly as the doping level increases from UD to OVD. The relaxation behaviors of ^{57}Fe - $(1/T_1T)$ for OPT and OVD respectively resemble those of ^{75}As -NMR- $(1/T_1T)$ for $\text{LaFeAsO}_{1-x}\text{F}_x$ with $x = 0.11$ and 0.14 .^{11,16)} In contrast, the relaxation behavior of ^{57}Fe - $(1/T_1T)$ for UD is considerably different from that of ^{75}As -NMR- $(1/T_1T)$ for the underdoped

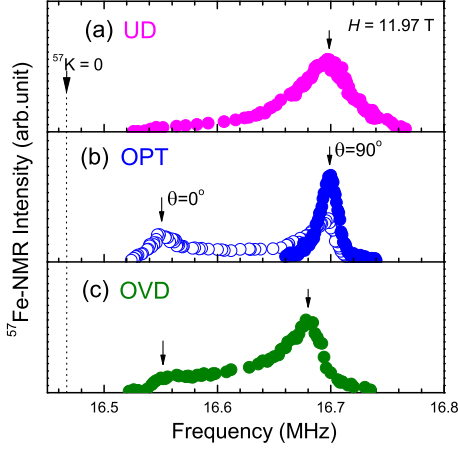


Fig. 2. (color online) ^{57}Fe -NMR spectra for (a) UD, (b) OPT, and (c) OVD of LaFeAsO_{1-y} at $H = 11.97$ T and 30 K. For OPT, which was oriented along the direction including the ab -plane, the spectra with a single narrow peak and two horn-shaped peaks respectively correspond to fields parallel and perpendicular to the direction including the ab -plane. The broad spectrum of UD (a) with the field parallel to the ab -plane originates from the inhomogeneous distribution of the ^{57}Fe Knight shift, which is caused by the phase separation into SC and magnetic domains at a microscopic scale in UD close to an AFM phase (see text). The spectrum of OVD (c), which was not oriented, indicates an asymmetric powder pattern due to the anisotropy of the ^{57}Fe Knight shift.

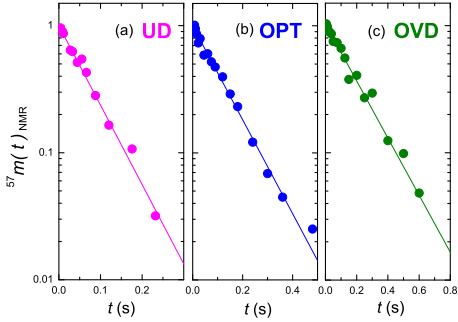


Fig. 3. (color online) Recovery curves of ^{57}Fe nuclear magnetization in the normal state at $T = 80$ K and $H = 11.97$ T for (a) UD, (b) OPT, and (c) OVD of LaFeAsO_{1-y} . In the entire range of T , the recovery curves are almost uniquely fitted by $^{57}m(t)_{\text{NMR}}$, as indicated by solid lines.

$\text{LaFeAsO}_{1-x}\text{F}_x$ with $x = 0.04$, which is enhanced upon cooling.^{11, 16} In order to reconcile why the T dependence of $1/T_1T$ for the present ^{57}Fe -NMR differs from the previous results obtained by ^{75}As -NMR measurements, in the next section we discuss with the ^{75}As -NMR T_1 measurements on the same samples as those in ^{57}Fe -NMR study.

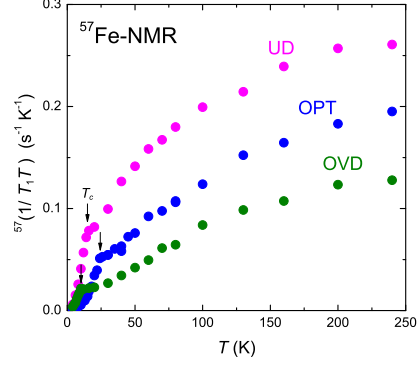


Fig. 4. (color online) T dependence of ^{57}Fe - $(1/T_1T)$ for LaFeAsO_{1-y} . In the normal state, $1/T_1T$ decreases significantly upon cooling for all samples, and the magnitude of $1/T_1T$ decreases markedly as the doping level increases when going from UD to OVD. The relaxation behaviors of ^{57}Fe - $(1/T_1T)$ for OPT and OVD respectively resemble those of ^{75}As -NMR- $(1/T_1T)$ for $\text{LaFeAsO}_{1-x}\text{F}_x$ with $x = 0.11$ and 0.14 .^{11, 16} In contrast, the relaxation behavior of ^{57}Fe - $(1/T_1T)$ for UD is considerably different from that of ^{75}As -NMR- $(1/T_1T)$ for the underdoped $\text{LaFeAsO}_{1-x}\text{F}_x$ with $x = 0.04$, which is enhanced upon cooling.^{11, 16}

3.2 ^{75}As -NMR/NQR studies on LaFeAsO_{1-y}

Figures 5(a)-5(c) respectively show the ^{75}As -NMR spectra at 30 K and $H = 11.97$ T for UD, OPT, and OVD of LaFeAsO_{1-y} . The sharp peak at approximately $f \sim 87.6$ MHz for all samples originates from the central transition ($I = +1/2 \leftrightarrow -1/2$) in the field parallel to the ab -plane ($\theta = 90^\circ$). The spectrum of OVD (c), which was not oriented, indicates an asymmetric powder pattern due to the anisotropy of the ^{75}As Knight shift. Note that the resonance frequency for $\theta = 90^\circ$ is almost invariant for all samples, in contrast with that in the ^{57}Fe -NMR spectra indicated in Fig. 2. This is because that the ^{75}As Knight shift is smaller than the ^{57}Fe Knight shift.

The recovery curve of ^{75}As nuclear magnetization ($I = 3/2$) obtained by the ^{75}As -NMR measurement is expressed by the following theoretical curve:

$$^{75}m(t)_{\text{NMR}} = 0.1 \exp\left(-\frac{t}{T_1}\right) + 0.9 \exp\left(-\frac{6t}{T_1}\right).$$

As shown in Fig. 6(a), $^{75}m(t)_{\text{NMR}}$ can be fitted by a theoretical curve at high temperatures ($T \geq 160$ K) for all samples. For UD, however, since it cannot be reproduced by a single component of T_1 below $\sim 150 \pm 10$ K, as shown in Fig. 6(b), a long component (T_{1L}) and a short component (T_{1S}) are tentatively estimated by assuming the expression $^{75}m(t)_{\text{NMR}} \equiv A_S^{75}m_S(t)_{\text{NMR}} + A_L^{75}m_L(t)_{\text{NMR}}$. Here, A_S and A_L (with $A_S + A_L = 1$) are the respective fractions of domains with T_{1S} and T_{1L} . The respective A_S for UD, OPT, and OVD are 0.7–0.8, 0.3–0.4, and ~ 0 , revealing that the volume fraction of domains with T_{1S} is increased when a sample approaches an AFM order and/or a structural transition. It should be noted that the T_1 of OVD was almost uniquely determined from a single component over the entire T range, although the

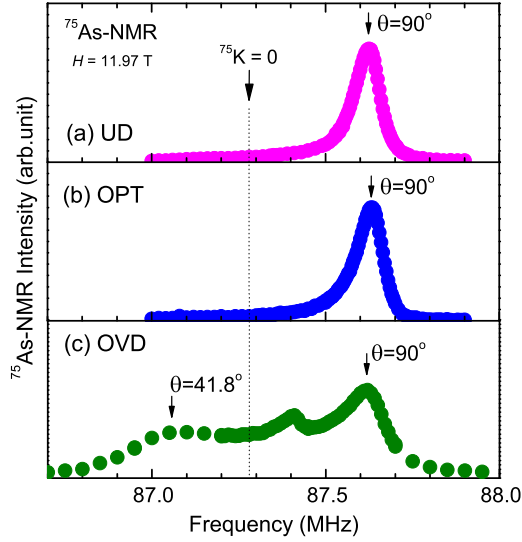


Fig. 5. (color online) ^{75}As -NMR spectra for (a) UD, (b) OPT, and (c) OVD of LaFeAsO_{1-y} at $H=11.97$ T and 30 K. The sharp peak at approximately $f \sim 87.6$ MHz originates from the central transition ($I = +1/2 \leftrightarrow -1/2$) in the field parallel to the ab -plane ($\theta = 90^\circ$). The asymmetric lineshape in the OVD sample is attributed to the unoriented powder sample. It is noteworthy that this resonance frequency for $\theta = 90^\circ$ does not vary for all the samples owing to the much smaller Knight shift at the As site than at the Fe site.

fraction of oxygen deficiencies is larger for OVD than for UD, revealing that the inhomogeneity of electronic states may be significant in UD close to an AFM phase and/or a structural transition.

Figure 7 shows the T dependences of ^{75}As -NMR ($1/T_1T$) at $H=11.97$ T along the ab -plane ($\theta = 90^\circ$) for all samples. In OVD, ^{75}As - $(1/T_1T)$ gradually decreases upon cooling to T_c , resembling the results of ^{57}Fe - $(1/T_1T)$ shown in Fig. 4. ^{75}As - $(1/T_1T)$ for UD and OPT also decrease upon cooling to their T_c similarly to the results of ^{57}Fe - $(1/T_1T)$. In fact, Fig. 8 reveals that the T dependence of ^{75}As - $(1/T_1T)$ is well scaled to that of ^{57}Fe - $(1/T_1T)$ with a ratio of $^{57}(1/T_1T)/^{75}(1/T_1T) \simeq 1.3$. This suggests that these ^{75}As -NMR- $(1/T_1)$ components reveal a normal-state property inherent to UD, OPT, and OVD. On the other hand, ^{75}As - $(1/T_1S T)$ for UD and OPT, which increase and stay a nearly constant upon cooling, respectively, are not scaled to ^{57}Fe - $(1/T_1T)$, as indicated in Fig. 8. These results indicate that UD and OPT may contain unknown phases in addition to Fe-based oxypnictide superconductors. Here, we remark that the relaxation behaviors of ^{75}As - $(1/T_1S T)$ for UD and OPT resemble those of $\text{LaFeAsO}_{1-x}\text{F}_x$ with $x = 0.04$ and 0.07 ,¹⁶ respectively.

In order to inspect whether or not the unknown phases are Fe-based oxypnictide phases, we measured ^{75}As -NQR T_1 for UD at the ^{75}As -NQR frequency inherent to LaFeAsO_{1-y} .¹⁸ Because the volume fraction of domains with T_{1S} is increased when a sample approaches an AFM phase and/or a structural transition, it is likely

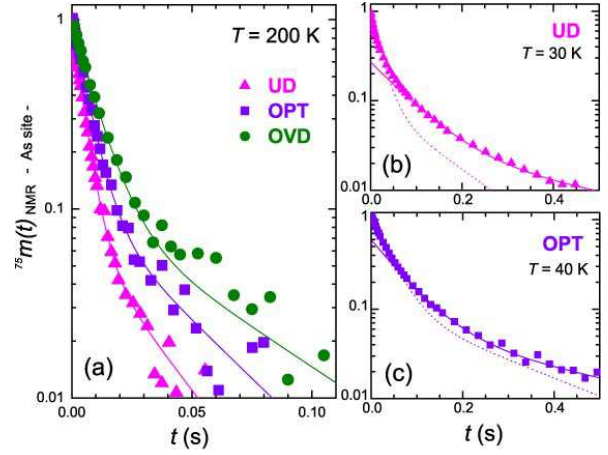


Fig. 6. (color online) Recovery curves of ^{75}As nuclear magnetization. (a) The curves are uniquely determined by the theoretical function $^{75}m(t)_{\text{NMR}}$ (solid lines) above ~ 160 K for all samples. However, below $\sim 150 \pm 10$ K, $^{75}m(t)_{\text{NMR}}$ cannot be reproduced by the theoretical curve in (b) UD and (c) OPT because of a phase separation (see text). The volume fraction with a short T_1 is increased when a sample approaches an AFM order and/or a structural transition.

that these domains arise from magnetic phases. In order to confirm this, we next present the relaxation behavior for the nondoped sample (ND).

3.3 Zero-field ^{75}As -NMR in nondoped LaFeAsO

In magnetically ordered materials, the NMR spectrum can be observed at a zero field, since an internal field H_{int} is induced by magnetically ordered moments. Figure 9 shows the ^{75}As -NMR spectra at a zero field in the AFM state at 2.2 K for nondoped LaFeAsO (ND). The very sharp NMR spectra of ND indicate the good quality of the sample. Two narrow spectra at 11.7 and 20.6 MHz can be simulated using the NQR frequency $\nu_Q = 8.8$ MHz and $H_{\text{int}} = 1.60$ T along the c -axis, as shown by the solid curve in the figure. Note that H_{int} at the As site is the off-diagonal pseudodipole field induced by the stripe-type AFM ordered moments in the ab -plane.¹⁹ Interestingly, $H_{\text{int}} = 1.60$ T for LaFeAsO is nearly equal to $H_{\text{int}} = 1.5$ T for BaFe_2As_2 .^{19,20}

The ^{75}As -NMR T_1 of ND, which was measured in the paramagnetic state in the range $T=150$ - 250 K at $H = 11.97$ T parallel to the ab -plane, was uniquely determined. ^{75}As -NMR spectra have been published elsewhere.¹⁸ The ^{75}As - $(1/T_1T)$ of ND is presented in Fig. 7, along with those of UD, OPT, and OVD. The ^{75}As - $(1/T_1T)$ of ND appears to be markedly enhanced toward the AFM ordering temperature $T_N \sim 145$ K, resembling the results of ^{139}La -NMR $1/T_1$.¹¹ This relaxation behavior differs from those for the SC phases in UD, OPT, and OVD, which exhibit a significant decrease upon cooling. In this context, the reason for the increase in ^{75}As - $(1/T_1S T)$ for UD upon cooling may be ascribed to the inclusion of some magnetic domains. We next focus on this issue.

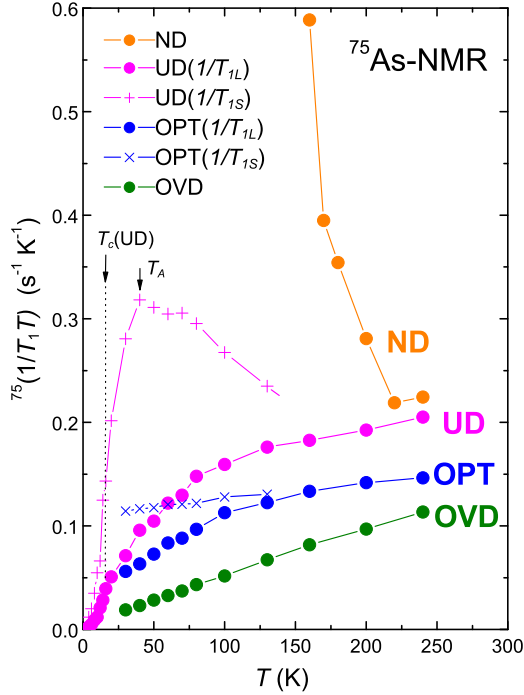


Fig. 7. (color online) T dependences of $^{75}\text{As-NMR}-(1/T_1T)$ for LaFeAsO_{1-y} at $H \sim 11.97$ T parallel to the ab -plane ($\theta = 90^\circ$). $^{75}\text{As}-(1/T_{1L}T)$ gradually decreases upon cooling to T_c in all samples, resembling the results of $^{57}\text{Fe}-(1/T_1T)$. On the other hand, $^{75}\text{As}-(1/T_{1S}T)$ for UD and OPT increase and stay a nearly constant upon cooling, respectively; neither of which are scaled to $^{57}\text{Fe}-(1/T_1T)$.

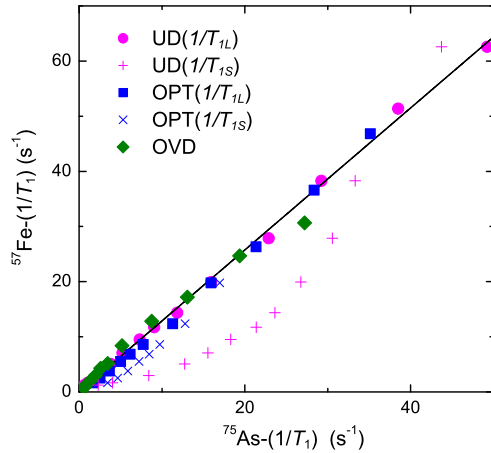


Fig. 8. (color online) Plot of $^{57}\text{Fe}-(1/T_1)$ versus $^{75}\text{As}-(1/T_1)$ with the implicit parameter of T between 30 and 240 K for UD, OPT, and OVD. The T dependence of $^{57}\text{Fe}-(1/T_1)$ is well scaled to that of $^{75}\text{As}-(1/T_1)$ for OVD and $^{75}\text{As}-(1/T_{1L})$ for UD and OPT with a ratio of $^{57}(1/T_1T)/^{75}(1/T_1T) \simeq 1.3$. However, $^{75}\text{As}-(1/T_{1S})$ for UD and OPT samples are not scaled to $^{57}\text{Fe}-(1/T_1)$, suggesting that an intrinsic property of SC phases can be probed through the result of $^{75}\text{As}-(1/T_{1L})$.

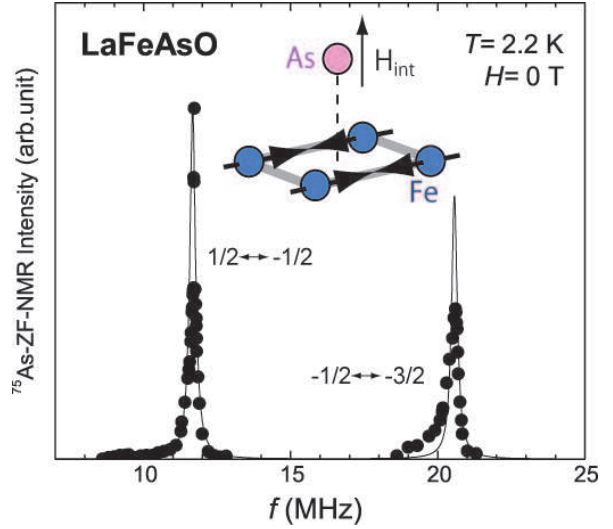


Fig. 9. (color online) Zero-field $^{75}\text{As-NMR}$ spectrum for non-doped LaFeAsO at 2.2 K. Two narrow spectra at 11.7 MHz (central peak) and 20.6 MHz (satellite peak) can be simulated using the NQR frequency $\nu_Q = 8.8$ MHz and $H_{int} = 1.60$ T at ^{75}As along the c -axis, as shown by the solid curve. Note that H_{int} at the As site is the off-diagonal pseudodipole field induced by the AFM moment at the Fe site, whose direction is in the ab -plane, which forms the stripe-type AFM structure.¹⁹⁾

4. Discussion

4.1 Phase separation in the underdoped sample (UD)

The observation of two components (T_{1S} and T_{1L}) of T_1 in UD indicates some local inhomogeneity in association with the density distribution of oxygen deficiencies. Namely, it is likely that magnetic domains are nucleated owing to its relatively low density of oxygen deficiencies in UD. The fraction A_S of magnetic domains in UD, which exhibits the increase in $1/T_{1S}$ upon cooling, is 0.7–0.8, revealing that the magnetic domains appear to be separated from the SC domains when the doping level approaches an AFM phase and/or a structural transition. Here we comment on why $^{57}\text{Fe-NMR-T}_1$ in UD was determined by an almost single component even though a phase separation into the magnetic and SC domains takes place. Figures 10(a) and 10(b) respectively show $^{57}\text{Fe-NMR}$ and $^{75}\text{As-NMR}$ spectra for UD. Figure 10(c) shows the T dependence of the linewidth of both spectra. The ^{57}Fe linewidth increases significantly upon cooling below 130–150 K, whereas the ^{75}As linewidth increases gradually below 130–150 K. These results suggest that a tiny magnetic moment is induced at the Fe site in the magnetic domains below 130~150 K. The further increase of ^{75}As linewidth is seen below $T_A \sim 40$ K, suggesting that the increase of magnetic-domain size upon cooling stabilizes the static short-range magnetic order (SRMO) in UD, which is corroborated by the observation of the peak in $1/T_{1S}$ at T_A shown in Fig. 7. $^{57}\text{Fe}-(1/T_1T)$ was measured at the center of the broad $^{57}\text{Fe-NMR}$ spectra that arises predominantly from the SC domains and hence was almost uniquely determined. On the other hand, since the broadening of the $^{75}\text{As-NMR}$ spectra is much less than that of the $^{57}\text{Fe-NMR}$ spectra and hence the center of the $^{75}\text{As-NMR}$ spectra arises

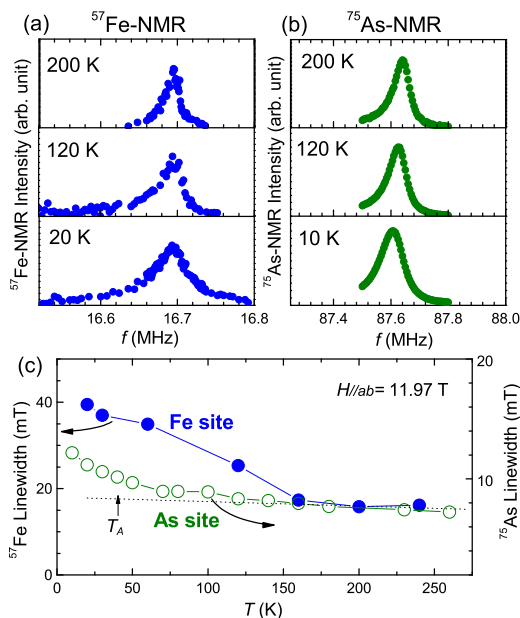


Fig. 10. (color online) T dependence of (a) ^{57}Fe -NMR and (b) ^{75}As -NMR spectra for the oriented UD sample in the field $H = 11.97$ T parallel to the ab -plane. (c) T -dependence of the linewidth of these ^{57}Fe -NMR and ^{75}As -NMR spectra. It is noteworthy that the broadening of the NMR spectra is more significant at the Fe site than at the As site.

from both the magnetic and SC domains, ^{75}As - $(1/T_1T)$ includes two components, $1/T_{1S}$ and $1/T_{1L}$, corresponding to the magnetic and SC domains, respectively. Note that similar results were also reported in previous works on underdoped $\text{LaFeAsO}_{1-x}\text{F}_x$ ($x = 0.04$),^{11,16} in which it was claimed that T_A corresponds to the maximum of resistivity, implying the crossover from a bad metal to a somewhat better metal. We consider that the tiny moments induced in the magnetic domains below ~ 150 K may develop SRMO below T_A . Interestingly, the $1/T_{1S}$ of the magnetic domains decreases markedly below T_c , as shown in Fig. 7, which is presumably due to an SC proximity effect in association with the mixture of magnetic and SC domains. In this context, ^{57}Fe -NMR studies play a vital role in deducing the intrinsic normal-state properties of SC domains in Fe-based superconductors.

4.2 Phase diagram of LaFeAsO_{1-y}

The phase diagram of LaFeAsO_{1-y} in Fig. 1 shows the evolution from AFM to SC as a function of the a -axis length, which becomes shorter as oxygen deficiencies are introduced into the LaO layer. As a result of the systematic ^{57}Fe -NMR and ^{75}As -NMR measurements, we reveal the phase transition between AFM and SC as a function of oxygen deficiencies in LaFeAsO_{1-y} , as illustrated in Fig. 11. As the oxygen deficiencies are increased when going from UD to OVD, the fraction of magnetic domains becomes smaller in OPT and disappears in OVD, since their spatial distribution of electronic states becomes less prominent. The AFM order in most mother materials of Fe pnictides takes place slightly below the

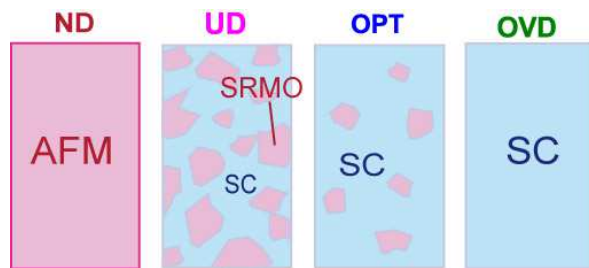


Fig. 11. (color online) Illustration of the phase separation into magnetic and SC domains in UD and OPT. As oxygen deficiencies are increased when going from UD to OVD, the fraction of magnetic domains becomes smaller in OPT and disappears in OVD, since their spatial distribution of electronic states becomes less prominent. In UD, short-range magnetic order (SRMO) in the magnetic domain is suggested from the line broadening of NMR spectra. However no such broadening of the spectra was confirmed for OPT, probably due to the very small internal field.

temperature of the first-order structural phase transition from tetragonal to orthorhombic.^{7,21,22} Accordingly, it is likely that the local inhomogeneity of oxygen deficiencies in UD is responsible for the phase separation into magnetic and SC domains. The features presented here resemble the phase diagram of $\text{LaFeAsO}_{1-x}\text{F}_x$ revealed by μSR .²¹ A phase separation has also been reported for the sample near the phase boundary between the AFM and SC states.²³

4.3 Normal-state properties of electron- and hole-doped Fe pnictides

Finally, we compare the normal-state properties of electron-doped LaFeAsO_{1-y} and hole-doped $\text{Ba}_{0.6}\text{K}_{0.4}\text{Fe}_2\text{As}_2$.^{14,15,24} Figure 12(a) shows the T dependences of ^{57}Fe - $(1/T_1T)$ in the SC domains of UD, OPT, and OVD along with that for $\text{Ba}_{0.6}\text{K}_{0.4}\text{Fe}_2\text{As}_2$.²⁴ In the case of electron-doped LaFeAsO_{1-y} , it is noteworthy that $(1/T_1T)$ decreases upon cooling for all superconducting samples, revealing that AFM fluctuations are not dominant, even approaching the AFM phase. By contrast, the $1/T_1T$ of the optimally hole-doped $\text{Ba}_{0.6}\text{K}_{0.4}\text{Fe}_2\text{As}_2$ markedly increases upon cooling to T_c . A recent theoretical work²⁵ appears to qualitatively explain this on the basis of a fluctuation-exchange approximation (FLEX) using an effective five-band Hubbard model; in electron-doped systems, $1/T_1T$ and spin susceptibility decrease significantly upon cooling, suggesting a band structure effect, that is, the existence of a high density of states slightly below the Fermi level. This is consistent with the experimental finding for electron-doped LaFeAsO_{1-y} that the Knight shift in OPT of LaFeAsO_{1-y} decreases upon cooling as well as $1/T_1T$.¹⁷ On the other hand, the T dependence of $1/T_1T$ is markedly enhanced down to T_c in hole-doped $\text{Ba}_{0.6}\text{K}_{0.4}\text{Fe}_2\text{As}_2$, whereas the T dependence of the Knight shift remains constant in this T range.²⁴ These results do not appear to be understandable in terms of only a simple band-structure effect in this compound; the evolution of AFM spin fluctuations should additionally be taken into account.^{14,24,25}

On the basis of these results, we claim that $1/T_1T$ is

not always enhanced by AFM fluctuations close to an AFM phase in the underdoped SC sample of Fe pnictides. According to the theoretical study by Kuroki *et al.*,²⁶⁾ such AFM spin fluctuations may be attributed to the multiple spin-fluctuation modes arising from nesting across the disconnected Fermi surfaces. In this scenario, we deduce that a better nesting condition among the Fermi surfaces is realized in $\text{Ba}_{0.6}\text{K}_{0.4}\text{Fe}_2\text{As}_2$ than in LaFeAsO_{1-y} . Consequently, we remark that the crucial difference between the normal-state properties of LaFeAsO_{1-y} and $\text{Ba}_{0.6}\text{K}_{0.4}\text{Fe}_2\text{As}_2$ may originate from the fact that the relevant Fermi surface topologies are differently modified depending on whether electrons or holes are doped into the FeAs layers.

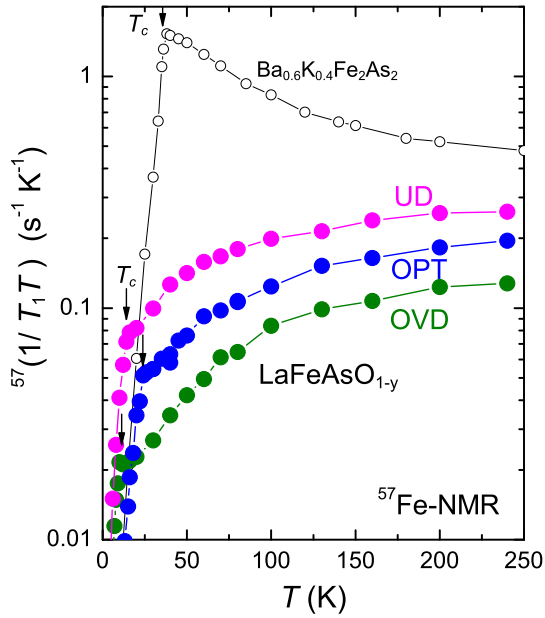


Fig. 12. (color online) T dependences of ^{57}Fe - $(1/T_1T)$ for electron-doped LaFeAsO_{1-y} and hole-doped $\text{Ba}_{0.6}\text{K}_{0.4}\text{Fe}_2\text{As}_2$ (cited from ref. 24). $1/T_1T$ in the electron-doped LaFeAsO_{1-y} decreases upon cooling, revealing that AFM spin fluctuations are not dominant, even approaching the vicinity of the AFM phase. By contrast, the $1/T_1T$ of the optimally hole-doped $\text{Ba}_{0.6}\text{K}_{0.4}\text{Fe}_2\text{As}_2$ markedly increases upon cooling to T_c .

In the superconducting state, as shown in Fig. 13, $1/T_1$ exhibits almost T^3 -like dependence below $T_c(H)$ regardless of the doping level of LaFeAsO_{1-y} in this T range, which was significantly different from the T^5 -like dependence of $\text{Ba}_{0.6}\text{K}_{0.4}\text{Fe}_2\text{As}_2$.²⁴⁾ As reported in a recent paper,²⁴⁾ the different behavior can be ascribed to the stronger coupling SC in $\text{Ba}_{0.6}\text{K}_{0.4}\text{Fe}_2\text{As}_2$ ($T_c^{\text{max}} = 38$ K) than in LaFeAsO_{1-y} ($T_c^{\text{max}} = 28$ K). Therefore, it is reasonable that the difference in the superconducting properties between LaFeAsO_{1-y} and $\text{Ba}_{0.6}\text{K}_{0.4}\text{Fe}_2\text{As}_2$ can be understood by the difference in their normal-state properties. In this context, we propose that the Fermi surface

topology, namely a nesting condition among the disconnected Fermi surfaces, may be responsible for SC characteristics inherent to each Fe-based superconductor.

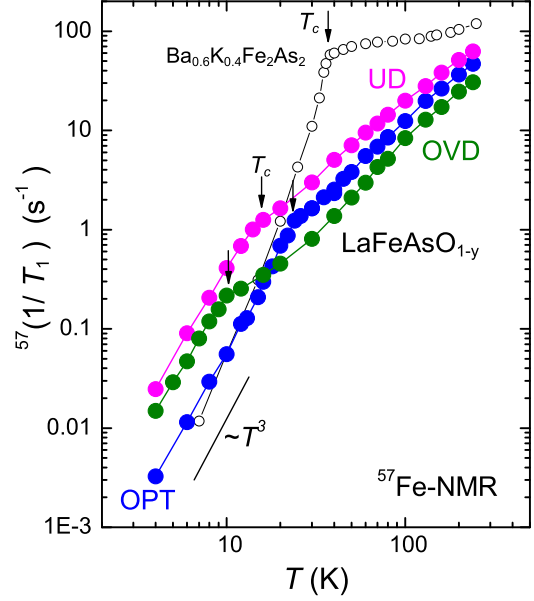


Fig. 13. (color online) T dependences of ^{57}Fe - $(1/T_1)$ for electron-doped LaFeAsO_{1-y} and hole-doped $\text{Ba}_{0.6}\text{K}_{0.4}\text{Fe}_2\text{As}_2$ (cited from ref. 24). $1/T_1$ exhibits almost T^3 -like dependence below $T_c(H)$ regardless of the doping level in LaFeAsO_{1-y} , which is significantly different from the T^5 -like dependence of $\text{Ba}_{0.6}\text{K}_{0.4}\text{Fe}_2\text{As}_2$.²⁴⁾ This suggests an intimate relationship between the superconducting properties and the normal-state properties.

5. Summary

Systematic ^{57}Fe -NMR and ^{75}As -NMR/NQR studies on the oxygen-deficient Fe-oxypnictide superconductor LaFeAsO_{1-y} have revealed a microscopic phase separation into SC and magnetic domains in an underdoped sample with $T_c=20$ K. As oxygen-deficiencies are increased when going from an underdoped sample to the overdoped sample, the fraction of magnetic domains becomes smaller and disappears in the overdoped sample, since the spatial distribution of electronic states becomes less prominent. It was demonstrated that $1/T_1T$ in the SC domains of the underdoped sample decreases markedly upon cooling to T_c for both the Fe and As sites as well as the results in the optimally doped and overdoped samples. As a result, we consider that the decrease of $1/T_1T$ upon cooling may be a common characteristic of the normal-state property of electron-doped LaFeAsO_{1-y} superconductors, regardless of the electron-doping level. This contrasts with the behavior in hole-doped $\text{Ba}_{0.6}\text{K}_{0.4}\text{Fe}_2\text{As}_2$, which exhibits a significant increase in $1/T_1T$ upon cooling. This crucial difference in the normal-state properties between LaFeAsO_{1-y} and

$\text{Ba}_{0.6}\text{K}_{0.4}\text{Fe}_2\text{As}_2$ may originate from the fact that relevant Fermi surface topologies are differently modified depending on whether electrons or holes are doped into the FeAs layers. From the comparison between the superconducting and normal-state properties, we propose that the Fermi surface topology, namely a nesting condition among the disconnected Fermi surfaces, may be responsible for SC characteristics inherent to each Fe-based superconductor. A remaining important issue is to investigate the correlation between the electronic structure and SC characteristics in various Fe-pnictide superconductors, which may lead to a general SC mechanism of Fe-based superconductors. Experiments to investigate this issue are now in progress.

Acknowledgements

This work was supported by a Grant-in-Aid for Specially Promoted Research (20001004) and by the Global COE Program (Core Research and Engineering of Advanced Materials-Interdisciplinary Education Center for Materials Science) from the Ministry of Education, Culture, Sports, Science and Technology (MEXT), Japan.

- 1) Y. Kamihara, T. Watanabe, M. Hirano, and H. Hosono: *J. Am. Chem. Soc.* **130** (2008) 3296.
- 2) H. Takahashi, K. Igawa, K. Arii, Y. Kamihara, M. Hirano, and H. Hosono: *Nature (London)* **453** (2008) 376.
- 3) Z. A. Ren, W. Lu, J. Yang, W. Yi, X. L. Shen, Z. C. Li, G. C. Che, X. L. Dong, L. L. Sun, F. Zhou, and Z. X. Zhao: *Chin. Phys. Lett.* **25** (2008) 2215.
- 4) H. Kito, H. Eisaki, and A. Iyo: *J. Phys. Soc. Jpn.* **77** (2008) 063707.
- 5) Z. A. Ren, G. C. Che, X. L. Dong, J. Yang, W. Lu, W. Yi, X. L. Shen, Z. C. Li, L. L. Sun, F. Zhou, and Z. X. Zhao: *Europhys. Lett.* **83** (2008) 17002.
- 6) J. Yang, Z. C. Li, W. Lu, W. Yi, X. L. Shen, Z. A. Ren, G. C. Che, X. L. Dong, L. L. Sun, F. Zhou and Z. X. Zhao: *Supercond. Sci. Technol.* **21** (2008) 082001.
- 7) C. de la Cruz, Q. Huang, J. W. Lynn, J. Y. Li, W. Ratcliff, II, J. L. Zarestky, H. A. Mook, G. F. Chen, J. L. Luo, N. L. Wang, and P. C. Dai: *Nature (London)* **453** (2008) 899.
- 8) C. H. Lee, H. Eisaki, H. Kito, M. T. Fernandez-Diaz, T. Ito, K. Kihou, H. Matsushita, M. Braden, and K. Yamada: *J. Phys. Soc. Jpn.* **77** (2008) 083704.
- 9) P. M. Shirage, K. Miyazawa, H. Kito, H. Eisaki, and A. Iyo: *Phys. Rev. B* **78** (2008) 172503.
- 10) T. Sato, S. Souma, K. Nakayama, K. Terashima, K. Sugawara, T. Takahashi, Y. Kamihara, M. Hirano, and H. Hosono: *J. Phys. Soc. Jpn.* **77** (2008) 063708.
- 11) Y. Nakai, K. Ishida, Y. Kamihara, M. Hirano, and H. Hosono: *J. Phys. Soc. Jpn.* **77** (2008) 073701.
- 12) K. Ahilan, F. L. Ning, T. Imai, A. S. Sefat, R. Jin, M. A. McGuire, B. C. Sales, and D. Mandrus: *Phys. Rev. B* **78** (2008) 100501(R).
- 13) F. Ning, K. Ahilan, T. Imai, A. S. Sefat, R. Jin, M. A. McGuire, B. C. Sales, and D. Mandrus: *J. Phys. Soc. Jpn.* **78** (2009) 013711.
- 14) H. Fukazawa, T. Yamazaki, K. Kondo, Y. Kohori, N. Takeshita, P. M. Shirage, K. Kihou, K. Miyazawa, H. Kito, H. Eisaki, and A. Iyo: *J. Phys. Soc. Jpn.* **78** (2009) 033704.
- 15) H. Mukuda, N. Terasaki, M. Yashima, H. Nishimura, Y. Kitaoka, and A. Iyo: *Physica C* **469** (2009) 559.
- 16) Y. Nakai, K. Ishida, Y. Kamihara, M. Hirano, and H. Hosono: *Phys. Rev. B* **79** (2009) 212506.
- 17) N. Terasaki, H. Mukuda, M. Yashima, Y. Kitaoka, K. Miyazawa, P. M. Shirage, H. Kito, H. Eisaki, and A. Iyo: *J. Phys. Soc. Jpn.* **78** (2009) 013701.
- 18) H. Mukuda, N. Terasaki, H. Kinouchi, M. Yashima, Y. Kitaoka, S. Suzuki, S. Miyasaka, S. Tajima, K. Miyazawa, P. M. Shirage, H. Kito, H. Eisaki, and A. Iyo: *J. Phys. Soc. Jpn.* **77** (2008) 093704.
- 19) K. Kitagawa, N. Katayama, K. Ohgushi, M. Yoshida, and M. Takigawa: *J. Phys. Soc. Jpn.* **77** (2008) 114709.
- 20) H. Fukazawa, K. Hirayama, K. Kondo, T. Yamazaki, Y. Kohori, N. Takeshita, K. Miyazawa, H. Kito, H. Eisaki, and A. Iyo: *J. Phys. Soc. Jpn.* **77** (2008) 093706.
- 21) H. Luetkens, H.-H. Klauss, M. Kraken, F. J. Litterst, T. Dellmann, R. Klingeler, C. Hess, R. Khasanov, A. Amato, C. Baines, M. Kosmala, O. J. Schumann, M. Braden, J. Hamann-Borrero, N. Leps, A. Kondrat, G. Behr, J. Werner, and B. Buchner: *Nat. Mater.* **8** (2009) 305.
- 22) H. Kotegawa, H. Sugawara, and H. Tou: *J. Phys. Soc. Jpn.* **78** (2009) 013709.
- 23) S. Takeshita, R. Kadono, M. Hiraishi, M. Miyazaki, A. Koda, Y. Kamihara, and H. Hosono: *J. Phys. Soc. Jpn.* **77** (2008) 103703.
- 24) M. Yashima, H. Nishimura, H. Mukuda, Y. Kitaoka, K. Miyazawa, P. M. Shirage, K. Kiho, H. Kito, H. Eisaki, and A. Iyo: *arXiv:0905.1896*.
- 25) H. Ikeda: *J. Phys. Soc. Jpn.* **77** (2008) 123707.
- 26) K. Kuroki, S. Onari, R. Arita, H. Usui, Y. Tanaka, H. Kontani, and H. Aoki: *Phys. Rev. Lett.* **101** (2008) 087004.